Indextron

Alexei Mikhailov[a] and Mikhail Karavay[b]
Institute of Control Problems, Russian Acad. of Sciences, Profsoyuznaya Street, 65, Moscow, Russia

Keywords: Pattern Recognition, Machine Learning, Neural Networks, Inverse Sets, Inverse Patterns, Multidimensional Indexing.

Abstract: How to do pattern recognition without artificial neural networks, Bayesian classifiers, vector support machines and other mechanisms that are widely used for machine learning? The problem with pattern recognition machines is time and energy demanding training because lots of coefficients need to be worked out. The paper introduces an indexing model that performs training by memorizing inverse patterns mostly avoiding any calculations. The computational experiments indicate the potential of the indexing model for artificial intelligence applications and, possibly, its relevance to neurobiological studies as well.

1 INTRODUCTION

Typically, pattern classification amounts to assigning a given pattern $\mathbf{x}$ to a class k out of K available classes. For this, K class probabilities $p_1(\mathbf{x}), p_2(\mathbf{x}),..., p_K(\mathbf{x})$ need to be calculated, after which the pattern $\mathbf{x}$ is assigned to the class k with a maximum probability $p_k(\mathbf{x})$ (Theodoridis, S. and Koutroumbas, K. , 2006). This paper avoids a discussion of classification devices, directly proceeding to finding class probabilities by a pattern inversion. Not only such approach cuts down on training costs, it might also be useful in studying biological networks, where details of intricate connectivity of neuronal patterns may not need to be unraveled. Then, for a given set of patterns, results of computational experiments can be compared to that of physical experiments.

For example, Tsunoda et al. (2001) demonstrated that "objects are represented in macaque inferotemporal (IT) cortex by combinations of feature columns". Figure 1 shows the images that were taken by Tsunoda et al. (2001) with a camera attached above a monkey's IT-region, where a piece of skull was removed. The anaesthetized monkey's IT-region responded to three cat-doll pictures, which were shown, in turn, with active spots marked by red, blue and green circles, correspondingly. The active spots appear on the IT-cortical map because the neurons under these spots exert increased blood flow, which is registered by an infrared camera. A clear set-theoretical inclusion pattern was observed, in which blue circles make a subset of red circles and green circles make a subset of blue circles.

This paper describes an experiment, where similar real cat pictures were shown to an indexing model referred to as the indextron. The outcomes are presented in (Figure1, IM) and annotated in the section Results, points 1.

Also, a comparative performance of the indextron versus artificial neural networks and decision functions was tested against benchmark datasets (see the section Results, points 2 - 3).

Comments are provided in the section 3. The indextron is considered in details in the Section 4.

2 RESULTS

1) A set-theoretical inclusion pattern, which is similar to that in Figure 1, IT, was observed in the memory of the indextron (Figure 1, IM). For that, this model was shown, in turn, complete and partial real cat images D, E, F retrieved from (Les Chats, 2010).

[a] https://orcid.org/0000-0001-8601-4101
[b] https://orcid.org/0000-0002-9343-366X

Mikhailov, A. and Karavay, M.
Indextron.
DOI: 10.5220/0010180301430149
In *Proceedings of the 10th International Conference on Pattern Recognition Applications and Methods (ICPRAM 2021)*, pages 143-149
ISBN: 978-989-758-486-2

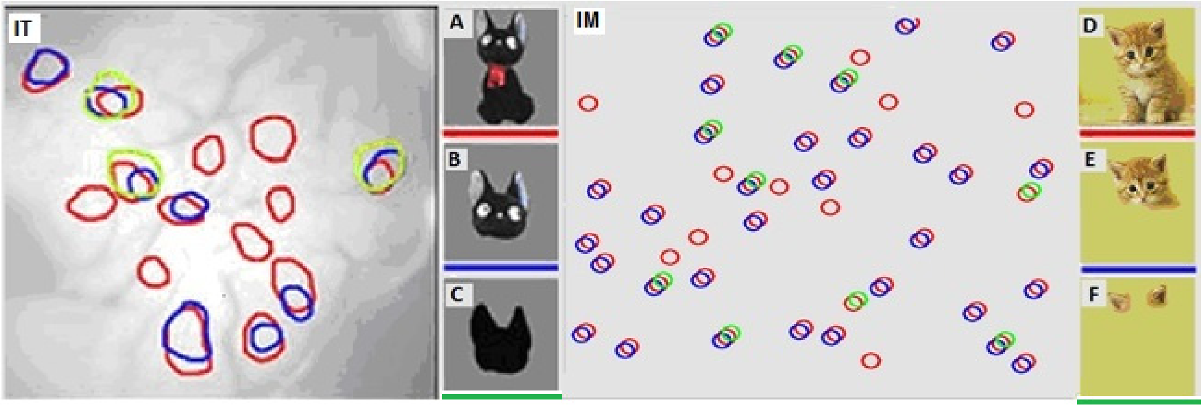

Figure 1: Activity in IT-region of a monkey and in the indextron memory (IM): **(IT)** The encircled areas were activated in IT-region of a monkey by cat-doll pictures. (**A**) Full cat-doll picture activated read areas. (**B**) Head cat-doll picture activated blue areas. (**C**) Head contour cat-doll picture activated green areas. **(IM)** Activity elicited in the model (a part of indextron memory is shown). (**D**) Full real cat picture activated read circles in IM. (**E**) Head picture activated blue areas in IM. (**F**) Ears activated green areas in IM. A clear set-theoretical inclusion pattern, where green circles are subsets of blue circles that are, in turn, subsets of red circles, is observed in both the IT-region and the model.

Table 1: Neural network versus indexing classifier.

Classifier	Accuracy (%)	Training (sec)	Hardware & Libraries
4 layer neural network *) Layers: Flatten, Dropout, Dense (256 neurons, ReLu activation function), Dense (10 neurons, softmax)	85.3	900	AMD Ryzen 5 3600, Python, Nvidia GeForce GTX 1660 Super, TensorFlow, Keras, cuDNN
Indextron	82.87	16	AMD Ryzen 5 3600, Python

*) For feature extraction, the convolutional neural network VGG16 from the web-site KERAS (2019) had been pre-trained on the ImageNet database (2016). Next, VGG16 was trained on 50000 grey level 32x32 images (10 categories) from the CIFAR-10 dataset providing 512 features per image. Finally, 512 x 50000 features were used for training both a 4-layer neural network and the indextron. For testing, 10000 images (512 x 10000 features) from the above dataset were classified using both the 4- layer neural network and the indextron.

2) CIFAR – 10 dataset (Krizhevsky et al, 2009) was used for testing the indextron against artificial neural networks. It was shown that the indextron reduced the training time by the factor of 50 in comparison to a 4-layer neural network (ref. to Table 1).

3) The indextron's performance against decision functions was tested with the CoverType dataset (Chang D., Canny J., 2014). It was shown that the indextron algorithm running on a 1.6 MHz CPU outperformed by a factor of 2 a much more powerful 4-GPU NVidia platform (ref. to Table 2).

3 DISCUSSION

1) The structure of the indextron algorithm resembles that of a back-of-the-book index. If the observed similarity of responses between the indextron and a biological cortical region is not a coincidence, then it might be possible to suggest that cortical regions work similar to indexing systems, where input features serve as keywords activating outcomes with little or no arithmetic.

2) The fact that at a competitive 85% accuracy, a mundane 2-core CPU outperforms in terms of throughput a much more powerful 4-GPU, 8-core CPU platform can be explained by the simplicity of the indextron algorithm, which does not involve any floating-point operation, multiplications and adjustable coefficients.

3) Figure 1, IT, shows only a 10% sub-area of active model area, - the sub-area, which fits the image.
Nonetheless, the inclusion relationship holds throughout the entire area.

Table 2: Time and accuracy of classifiers at train / test samples 290506 / 290506 Cover Type dataset division.

Platform	Method	Training Time (sec)	Accuracy %
4GPU (NVidia GT X-690 64GB RAM 8-core CPU at 2.2 GHz	SkiKit	138.17	87.7
	CudaTree	30.47	96.0
	BiDMachRF	67.27	71.0
Dual-core CPU at 1.6MHz 3GB RAM	Indextron	16*	90

4) Experiments with the indextron suggest that two monkeys looking at the same pictures may elicit different active spot arrangements in their IT-region as they most probably learnt their visual experiences in different circumstances.

4 MATERIALS AND METHODS

4.1 Feature Extraction

Sets of local features were used to represent real cat's images from (Les Chats, 2010) (see Figure 1, (D, E, F)). Each color image was converted to a grey level image that was subject to edge detection followed by thinning out a list of edge points. For each remaining edge point, a histogram of distances from a current point to its 20 nearest neighbors was created to represent this point's vicinity by a feature vector $\mathbf{x} = (x_1, x_2, ..., x_N)$ Next, this vicinity was classified in an unsupervised fashion by the indextron model, where each active vicinity was represented by a cell on a two-dimensional memory plane. Since there does not exist a one-to-one mapping between an N-dimensional ($N > 2$) space and a two-dimensional plane, the active cells were randomly placed on the plane on a first-come-first-occupy basis (shown by circles on Figure. 1, (IT)). Colors of the circles represent 2nd level classes (body, head, and ears), where a 2nd level class was assigned a red, blue or green color, respectively.

2nd level classifier takes as its input a histograms of 1st level classes, i.e., a histograms of vicinity classes.

4.2 Pattern Classification

This paper introduces an indexing classifier referred to as the indextron. The indextron comprises a number of identical levels. Each level takes in as its input either a feature vector or a feature set and returns an index that represents the input's class. Once a set of indexes has been accumulated, a histogram of indexes can be used as an input for the next level, which returns its output index that represents a meta-class of first level inputs. And so on "up to infinity". A single level classification problem can be summarized in strict mathematical terms as follows.

Let all variables be integers and K pattern classes be represented by a collection of K vectors

$$x_{k,1},...,x_{k,n},...,x_{k,N},\ k = 1,2,...,K \qquad (1)$$

in N-dimensional space, such that all vector components are restricted as $0 \pounds\ x_{k,n} < X$. It is also assumed that the Chebyshev distance between any two vectors k, j is greater than R, that is, any two vectors differ in at least one component

$$''k, j\ \$n:\ |x_{k,n} -\ x_{j,n}|\ > R$$

Problem: Given an unknown vector $x(n),\ n = 1,2,...,N$, find its class, that is, find the vector k from the given collection, such that the Chebyshev distance between these two vectors is less than R

$$''n\ |x(n) -\ x_{k,n}|\ \pounds\ R$$

Solution: Consider the indexed sets $\{k\}_{x,n}$ defined as

$$\begin{aligned} &\{k\}_{x,n} = \ \{k:\ |x(n) -\ x_{k,n}|\ \pounds\ R\} \\ &0 \pounds\ x < X,\ n = 1,2,...,N \end{aligned} \qquad (2)$$

The solution can be found as the class index k from the intersection

$$\bigcap_{n=1}^{N} \bigcup_{r=-R}^{R} \{k\}_{x(n)+r,\, n} \qquad (3)$$

Note 1: The intersection (3) is empty if $\max_k H(k) < N$, where the histogram $H(k)$ is calculated as follows

$$\forall n, \forall r: \ |r| \le R, \ \forall k \in \{k\}_{x(n)+r,\, n}$$

$$\text{calculate } H(k) = H(k) + 1$$

Note 2: If the intersection (3) is not empty then there always exists a single solution. This statement is a consequence of the following properties of the pattern transform. Each dimension n

- contains exactly K distinct class indexes

$$\sum_{x=0}^{X-1} |\{k\}_{x,n}| = K$$

- does not have intersecting sets:

$$\{k\}_{x,m} \cap \{k\}_{y,n} = \emptyset$$

Note 3: If the intersection (3) is empty then, on learning, the original collection (1) is to be expanded by the vector $x(n),\ n = 1,2,...,N$, that is assigned to a new class $K^{+} = K + 1$. However, the collection (1) does not physically exist in the memory. Instead, the memory is populated with sets (2).

Note 4: Whereas elements $x_{k,n}$ of vectors (1) constitute the pattern features, the elements of sets $\{k\}_{x,n}$ represent pattern classes. The sets (2) are referred to as the inverse patterns or columns. If the intersection (3) is empty then, on learning, the columns are updated as

$$\{k\}_{x,n} = \{k\}_{x,n} \cup K^{+}, \ n = 1,2,...,N$$

For an example, refer to Figure 2.

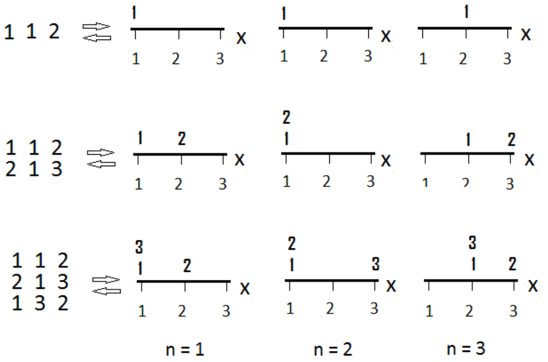

Figure 2: Three iterations involving growing columns that graphically represent inverse patterns.

For this example, the indexes 1, 2, 3 of the patterns $(1,1,2)_1, (2,1,3)_2, (1,3,2)_3$ are stored in respective columns. For instance, $\{k\}_{x=3,\, n=2} = \{3\}$ $\{k\}_{x=1,\, n=1} = \{3,1\}$, $\{k\}_{x=1,\, n=3} = \emptyset$.

A notion of inverse patterns was introduced in (Mikhailov, A. et al., 2017) and further discussed in (Mikhailov, A. and Karavay, M., 2019). This notion is related to inverse files technology used in Google search engine (Brin, S. and Page, L., 1998) and in the bag-of-words approach (Sivic, J. and Zisserman, A., 2009). Whereas the latter approach recasts visual object retrieval as text retrieval, the indextron evaluates class probabilities of visual objects and other objects such as sets, etc. by analyzing inverse patterns of numeric features. For example, the features *a, b, c* from indexed sets $\{a, b\}_1, \{b, c\}_2$ are associated with the inverse sets $\{1\}_a, \{1, 2\}_b, \{2\}_c$, which indicate that the feature *a* belongs only to the set 1, the feature *b* belongs to both the set 1 and the set 2, whereas the feature *c* belongs only to the set 2.

For patterns, inverse pattern of a feature x is a set $\{k\}_x$ of classes k associated with this feature. So, for two classes A, A, **A** and T, **T**, the feature "horizontal line" takes part in both A- and T-classes whereas the feature "vertical line" takes part only in class T: $\{A,T\}_{0^\circ}$, $\{T\}_{90^\circ}$.

The value of R in the transform (2) controls a generalization capability of the classifier. Although the total number K of classes grows as new patterns arrive, the rate of growth is inverse proportional to generalization radius R.

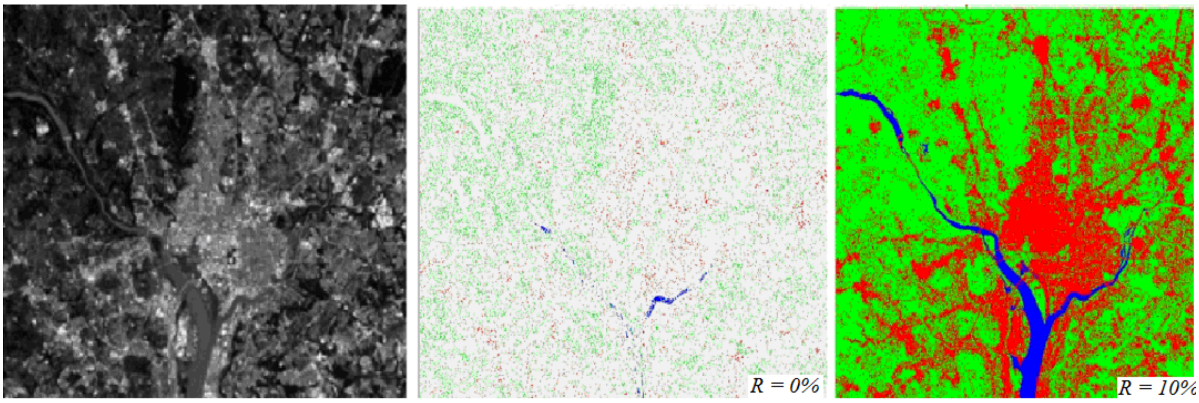

Figure 3: Image segmentation.

4.3 Generalization Radius

In accordance with the definition (1), any feature change $x_1 + \Delta_1,\ x_2 + \Delta_2, \ldots,\ x_N + \Delta_N$, such that a variation $|\Delta_n| \le R,\ n = 1,2,..,N$, does not affect a pattern's class. An influence of the radius R is shown on Figure 3. For this application, the pixels of the left-hand side image are to be classified into 3 classes (water, vegetation, urban development). Each pixel of the left-hand-side is represented by a 4-dimensional vector comprising components in the 256-level range in red, green, blue and infrared spectra (only one component is shown). For original images, refer to Gonzalez, R. and Woods, R. (2008).

The image at the center shows the segmentation result at $R = 0$, where most pixels remain unclassified. The right-hand side image shows a high quality image segmentation at $R = 10\%$ of 256-brightness range.

4.4 Indextron Architecture

The main parameters of the indextron are: the pattern dimensionality N, the feature range X and the maximum number K of classes that can be created by the classifier. In other words, the indextron comprises N groups of addresses, where each group n contains X addresses ranging from 0 to $X - 1$. Typically, the normalized integer feature range X is $[0,1,2,...,255]$. Each address $(x,\ n)$ is a gateway to the inverse pattern $\{k\}_{x,\,n}$ referred to as column (Figure 4).

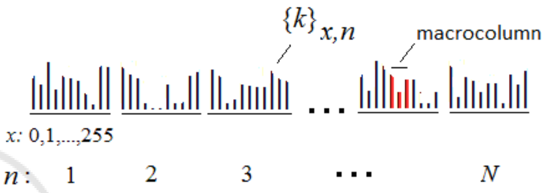

Figure 4: N groups of indextron columns presenting a cardinality distribution of inverse patterns.

Each column holds class indexes k, so that a column height is equal to the cardinality of the corresponding inverse pattern. A macro-column is defined by the generalization radius R and contains the neighboring columns with addresses from the interval $[x - R,\ x + R]$.

In Figure 4, inverse patterns are shown as N groups of columns, each group containing X columns. The average column height h does not account for 0-height columns. With classification computational complexity of $O(hN)$, a flat cardinality distribution of the inverse patterns is preferable to a delta-like distribution.

A parallel processing of N column groups can be implemented in a FPGA-chip, which leads to a practically instantaneous learning. A memory that needs to be allocated to column groups can be arrange in three ways, that is, (a) static columns, (b) dynamically allocated columns, (c) iterated one-dimensional maps (Dmitriev A. et al., 1991; Andreev et al., 1992). These methods would require KXN, $2KN$ and KN memory cells, respectively. The method (c) makes possible an FPGA-implementation of the $(K,\ X,\ N)$ = (512, 256, 1024) indextron with a 1,44 MB chip (Figure 5).

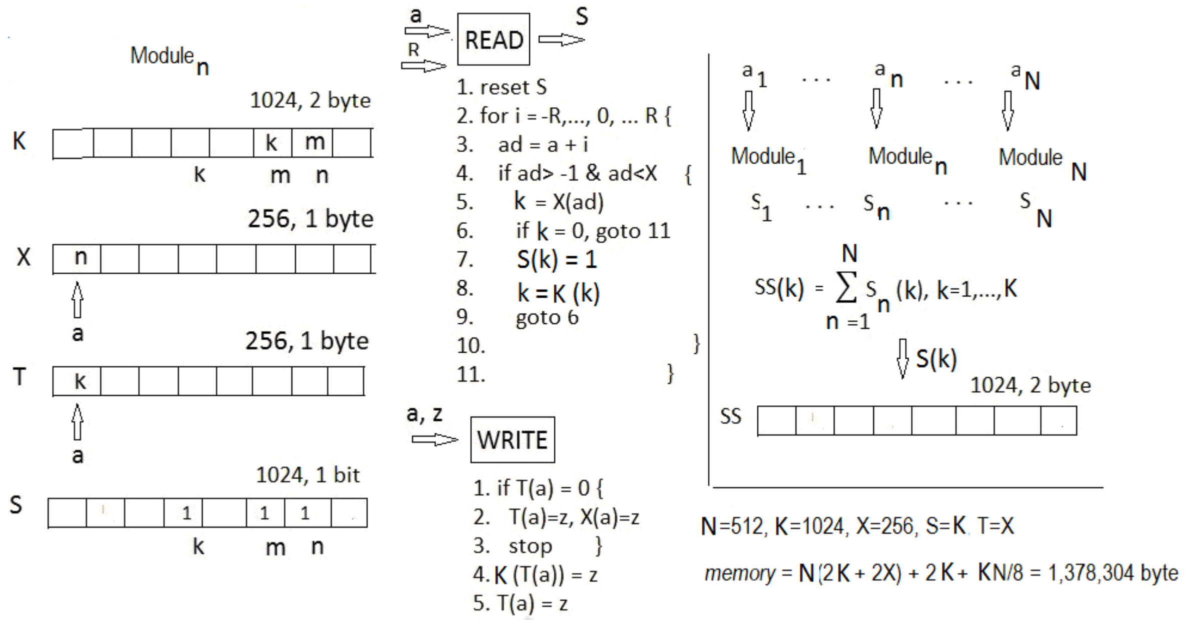

```
1. reset S
2. for i = -R,..., 0, ... R {
3.    ad = a + i
4.    if ad> -1 & ad<X    {
5.       k = X(ad)
6.       if k = 0, goto 11
7.       S(k) = 1
8.       k = K (k)
9.       goto 6
10.                        }
11.                     }
```

```
1. if T(a) = 0 {
2.  T(a)=z, X(a)=z
3.  stop    }
4. K (T(a)) = z
5. T(a) = z
```

$$SS(k) = \sum_{n=1}^{N} s_n(k), \; k=1,\dots,K$$

Figure 5: Indextron conceptual diagram.

In this case the total memory can be divided into N groups of four arrays (N, X, T, S) plus the common array SS. The total memory M amounts to

$$M = K(2N + X + T + N/8) + 2N \text{ (byte)}$$

A normalized discrete feature range of $X = 256$ has been found to be sufficient for most pattern recognition applications meaning that both float point features and integer features can be converted to 256 discrete levels without sacrificing an overall accuracy.

In such implementation scheme N identical modules work in parallel. The component a_n of the feature vector $a_1,\dots,a_n,\dots,a_N$ serves as the address to the 256-byte array X of the n-th module.

On inference, the READ-code is executed (see Figure. 5). The module's output is a 1024-bit word S_n. Next, N outputs are to be summed up producing the 1024-element array SS, whose elements are represented by 2-byte words

$$SS(k) = \sum_{n=1}^{N} S(n), \; k = 1,2,\dots,K$$

This array contains a conditional class distribution.

On learning, the WRITE-code is executed. Again, the component a_n of the feature vector $a_1,\dots,a_n,\dots,a_N$ serves as the address to the 256-byte array X of the n-th module, where the class index z will be stored.

ACKNOWLEDGEMENTS

We thank Prof. Tanifuji, Riken Brain Science Institute, for the permission to reproduce the image of the IT-cortical region of a monkey (Figure 1, IT).

REFERENCES

Theodoridis S. & Koutroumbas K. (2006). *Pattern Recognition*, Academic Press (3rd edition).

Tsunoda K., Yamane Y., Nishizaki M., Tanifuji M., (2001). Complex objects are represented in macaque inferotemporal cortex by the combination of feature columns. In *Nat. Neurosci. 4 (8).pp.832-838. doi:10.1038/90547. PMID 11477430*

Les Chats. (2010). Retrieved from *http://chatsetchiens3005.kazeo.com/les-chats-a122215626*

Krizhevsky A., Nair V., Hinton G., (2009). CIFAR-10. Retrieved from *https://www.cs.toronto.edu/~kriz/cifar.html*

Chang D,. Canny J,. (2014). Optimizing Random Forests on GPU. *Tech. Report No. UCB/EECS-2014-2095.*

Retrieved from *http://www.eecs.berckeley.edu/Pubs/TechRprts/2014/Eecs-2014-205.html*

Keras (2019). Retrieved from *https://keras.io*

Imagenet (2016). Retrieved from *http://image-net.org*

Mikhailov A., Karavay M., Farkhadov M. (2017). Inverse Sets in Big Data Processing. In *Proceedings of the 11th IEEE International Conference on Application of Information and Communication Technologies (AICT2017, Moscow). M.: IEEE, Vol. 1 https://www.researchgate.net/publication/321309177_Inverse_Sets_in_Big_Data_Processing*

Mikhailov A.and Karavay M. (2019). Pattern Recognition by Pattern Inversion. In *Proceedings of the 2nd International conference on Image, Video Processing and Artificial Intelligence, Shanghai, China.* SPIE Digital Library V.11321.

Brin S.and Page L. (1998). The Anatomy of a large-scale hypotextual web search engine. In *Computer Networks and ISDN Systems Volume 30, Issues 1–7.* Stanford University, Stanford, CA, 94305, USA. Retrieved from *https://doi.org/10.1016/S0169-7552(98)00110-X*

Sivic J., Zisserman A. (2009). Efficient visual search of videos cast as text retrieval. In *IEEE Transactions on Pattern Analysis and Machine Intelligence Volume: 31, Issue: 4. doi***:** *10.1109/TPAMI.2008.111*

Gonzales R. & Woods R., (2008). *Digital Image Processing.* Pearson Prentice Hall (3rd edition). *http://www.imageprocessingplace.com/root_files_V3/image_databases.htm*

Dmitriev A., Panas A., Starkov S. (1991). Storing and recognizing information based on stable cycles of one-dimentional maps. In *Phys. Lett.* .

Andreev Y., Dmitriev A., Chua L, Wu C. (1992). Associative and random access memory using one-dimensional maps. In *International Journal of Bifurcation and Chaos vol.2, No 3.* World Scientific Publishing Company.